International Journal of Nanomedicine

Dovepress
open access to scientific and medical research

Open Access Full Text Article

ORIGINAL RESEARCH

Highly effective antiangiogenesis via magnetic mesoporous silica-based siRNA vehicle targeting the VEGF gene for orthotopic ovarian cancer therapy

This article was published in the following Dove Press journal:
International Journal of Nanomedicine
31 March 2015
Number of times this article has been viewed

Yijie Chen[1,2,*]
Xinran Wang[3,4,*]
Ting Liu[3,4]
Ding Sheng-zi Zhang[1,2]
Yunfei Wang[3,4]
Hongchen Gu[1,2]
Wen Di[3,4]

[1]State Key Laboratory of Oncogenes and Related Genes, Clinical Stem Cell Research Center, Ren Ji Hospital, School of Medicine, [2]School of Biomedical Engineering and Med-X Research Institute, [3]Department of Obstetrics and Gynecology, Ren Ji Hospital, School of Medicine, Shanghai Jiao Tong University, [4]Shanghai Key Laboratory of Gynecologic Oncology, Shanghai, People's Republic of China

*These authors contributed equally to this work

Correspondence: Hongchen Gu
State Key Laboratory of Oncogenes and Related Genes, School of Biomedical Engineering and Med-X Research Institute, Shanghai Jiao Tong University, 1954 Huashan Road, Shanghai 200030, People's Republic of China
Tel +86 21 6293 2904
Fax +86 21 6293 2907
Email hcgu@sjtu.edu.cn

Wen Di
Department of Obstetrics and Gynecology, Ren Ji Hospital, School of Medicine, Shanghai Jiao Tong University, 160 Pujian Road, Shanghai 200030, People's Republic of China
Tel +86 21 6838 3801
Fax +86 21 6838 3829
Email diwen163@163.com

Abstract: Therapeutic antiangiogenesis strategies have demonstrated significant antitumor efficacy in ovarian cancer. Recently, RNA interference (RNAi) has come to be regarded as a promising technology for treatment of disease, especially cancer. In this study, vascular endothelial growth factor (VEGF)-small interfering RNA (siRNA) was encapsulated into a magnetic mesoporous silica nanoparticle (M-MSN)-based, polyethylenimine (PEI)-capped, polyethylene glycol (PEG)-grafted, fusogenic peptide (KALA)-functionalized siRNA delivery system, termed M-MSN_VEGF siRNA@PEI-PEG-KALA, which showed significant effectiveness with regard to VEGF gene silencing in vitro and in vivo. The prepared siRNA delivery system readily exhibited cellular internalization and ease of endosomal escape, resulting in excellent RNAi efficacy without associated cytotoxicity in SKOV3 cells. In in vivo experiments, notable retardation of tumor growth was observed in orthotopic ovarian tumor-bearing mice, which was attributed to significant inhibition of angiogenesis by systemic administration of this nanocarrier. No obvious toxic drug responses were detected in major organs. Further, the magnetic core of M-MSN_VEGF siRNA@PEI-PEG-KALA proved capable of probing the site and size of the ovarian cancer in mice on magnetic resonance imaging. Collectively, the results demonstrate that an M-MSN-based delivery system has potential to serve as a carrier of siRNA therapeutics in ovarian cancer.

Keywords: antiangiogenesis, small interfering RNA, mesoporous silica nanoparticles, vascular endothelial growth factor, ovarian cancer

Introduction

The 5-year survival rate in patients with ovarian cancer remains low due to difficulties with regard to early diagnosis, drug resistance, and relapse after treatment.[1] Although surgical resection followed by chemotherapy has been considered standard treatment for more than 30 years, new strategies are needed to improve the tolerability and efficacy of treatment for ovarian cancer.[2] Various published studies have shown that angiogenesis is essential for tumor invasion and metastasis in ovarian cancer.[3,4] It is well known that vascular endothelial growth factor (VEGF) and the VEGF receptor comprise a critical signaling pathway in tumor angiogenesis.[5] Therefore, targeting this signaling pathway is one of the most promising strategies for antiangiogenesis therapy.[6] Attempts have been made to treat ovarian cancer using antiangiogenesis therapy, such as bevacizumab, in the clinical setting but side effects including thrombosis, proteinuria, and gastrointestinal perforation remain problematic.[7–11] Therefore, it is necessary to develop safer and more effective antiangiogenesis therapies for ovarian cancer.

submit your manuscript | www.dovepress.com
Dovepress
http://dx.doi.org/10.2147/IJN.S78774

With the knowledge that angiogenesis is necessary for the growth of ovarian cancer, researchers have sought to utilize angiogenesis-related small interfering RNA (siRNA) as a therapeutic strategy to abrogate tumors. RNA interference (RNAi) technology has been intensively evaluated in the treatment of ovarian cancer by knockdown of genes responsible for progression of cancer, which is achieved by delivery vectors.[12–17] Two research groups have reported highly effective suppression of ovarian tumor growth by construction of available vectors. One research group synthesized vasohibin-2 (associated with proangiogenic activity) siRNA and mixed it with atelocollagen to inhibit ovarian tumor growth.[15] Another group developed a bioreducible polymer for delivery of VEGF-siRNA using ultrasound, which had a similar ability to inhibit tumor growth.[17] Although these two siRNA delivery systems are useful for treating ovarian cancer via intratumoral injection, there remains a need for smarter vectors to enable systemic delivery of therapeutic siRNAs to improve their efficacy in the treatment of ovarian cancer and with the biocompatibility and safety needed for clinical application.

Mesoporous silica nanoparticles (MSNs) are a novel vehicle for delivering various drug molecules due to their unique mesoporous structure, large loading capacity,[18] readily controllable release,[19] and favorable biocompatibility.[20,21] In a previous study, we designed a novel magnetic mesoporous silica nanoparticle (M-MSN)-based siRNA delivery system for the treatment of lung cancer. Systemic application of VEGF-siRNA using this nanocarrier resulted in remarkable tumor suppression in both subdermal and orthotopic lung cancer models, and metastasis to the liver was also markedly reduced.[21] Therefore, VEGF was chosen as the target gene for the present study. The therapeutic potential of this nanocarrier was evaluated via a series of gene silencing experiments in a SKOV3 cell line, followed by systemic injection of the nanocarrier in orthotopic ovarian tumor-bearing mice (Figure 1). The results of our studies indicate that this nanocarrier effectively inhibited expression of the target gene at optimized concentrations without detectable cytotoxicity, and its therapeutic utility in vivo was corroborated by significant ovarian tumor suppression with negligible systemic side effects. Additionally, noninvasive imaging modality within the vector (each particle has a superparamagnetic core) was favored to assess siRNA delivery for the diagnosis or optimization of treatment windows by magnetic resonance imaging. Overall, this M-MSN-based siRNA delivery vehicle has demonstrated potential for use in the treatment of ovarian cancer.

Materials and methods

Materials

Cetyltrimethylammonium bromide, 3-aminopropyltriethoxysilane, tetraethyl orthosilicate, branched polyethylenimine (PEI, 25 kDa), and dimethyl sulfoxide were purchased from Sigma-Aldrich (Steinheim, Germany). N-hydroxysuccinimide-polyethylene glycol-maleimide (NHS-PEG-Mal, 3.5 kDa) was obtained from Jenkem Technology (Beijing, People's Republic of China). The 3-(4,5-dimethylthiazol-2-yl)-2,5-diphenyltetrazolium bromide (MTT) was obtained from Amresco (Solon, OH, USA), and 4′,6-diamidino-2-phenylindole was sourced from the Beyotime Institute of Biotechnology (NanTong, People's Republic of China). LysoTracker® Red DND was purchased from Invitrogen (Waltham, MA, USA). A quantikine human VEGF immunoassay kit was obtained from R&D Systems Inc. (Minneapolis, MN, USA). Anti-Ki67 rabbit polyclonal antibody and anti-CD31 rabbit polyclonal antibody were purchased from Abcam (Cambridge, MA, USA). Anti-VEGF rabbit polyclonal antibody was sourced from Merck Millipore (Billerica, MA, USA). Biotinylated second antibody, streptavidin peroxidase, and diaminobenzidine chromogen were purchased from Maixin-Bio (Fujian, People's Republic of China). Negative control (NC) siRNA (sense, 5′-UUC UCC GAA CGU GUC ACG UTT-3′; antisense, 5′-ACG UGA CAC GUU CGG AGA ATT-3′), fluorescein amidite-labeled NC siRNA (modified at the 5′ end of the sense strand), and VEGF siRNA (sense, 5′-GGA GUA CCC UGA UGA GAU CdTdT; antisense, 5′-GAU CUC AUC AGG GUA CUC CdTdT) were synthesized by GenePharma Co Ltd (Shanghai, People's Republic of China). KALA peptide with the sequence WEA KLA KAL AKA LAK HLA KAL AKA LKA CEA and fluorescently labeled cyanine dye 5.5 KALA were synthesized and purified by GL Biochem Ltd (Shanghai, People's Republic of China). A gene transfection kit (Lipofectamine™ 2000), Roswell Park Memorial Institute 1640 medium, penicillin-streptomycin, fetal bovine serum, and 0.25% trypsin-ethylenediaminetetraacetic acid solution were purchased from Invitrogen-Gibco (Waltham, MA, USA).

Preparation of M-MSN_siRNA@PEI-PEG-KALA

The procedure used to prepare M-MSN_siRNA@PEI-PEG-KALA is shown in Figure 1. The core of the nanocarrier contained M-MSNs, which were synthesized according to our previous study.[22] The siRNA loading experiment was then performed in accordance with the established approach.[23]

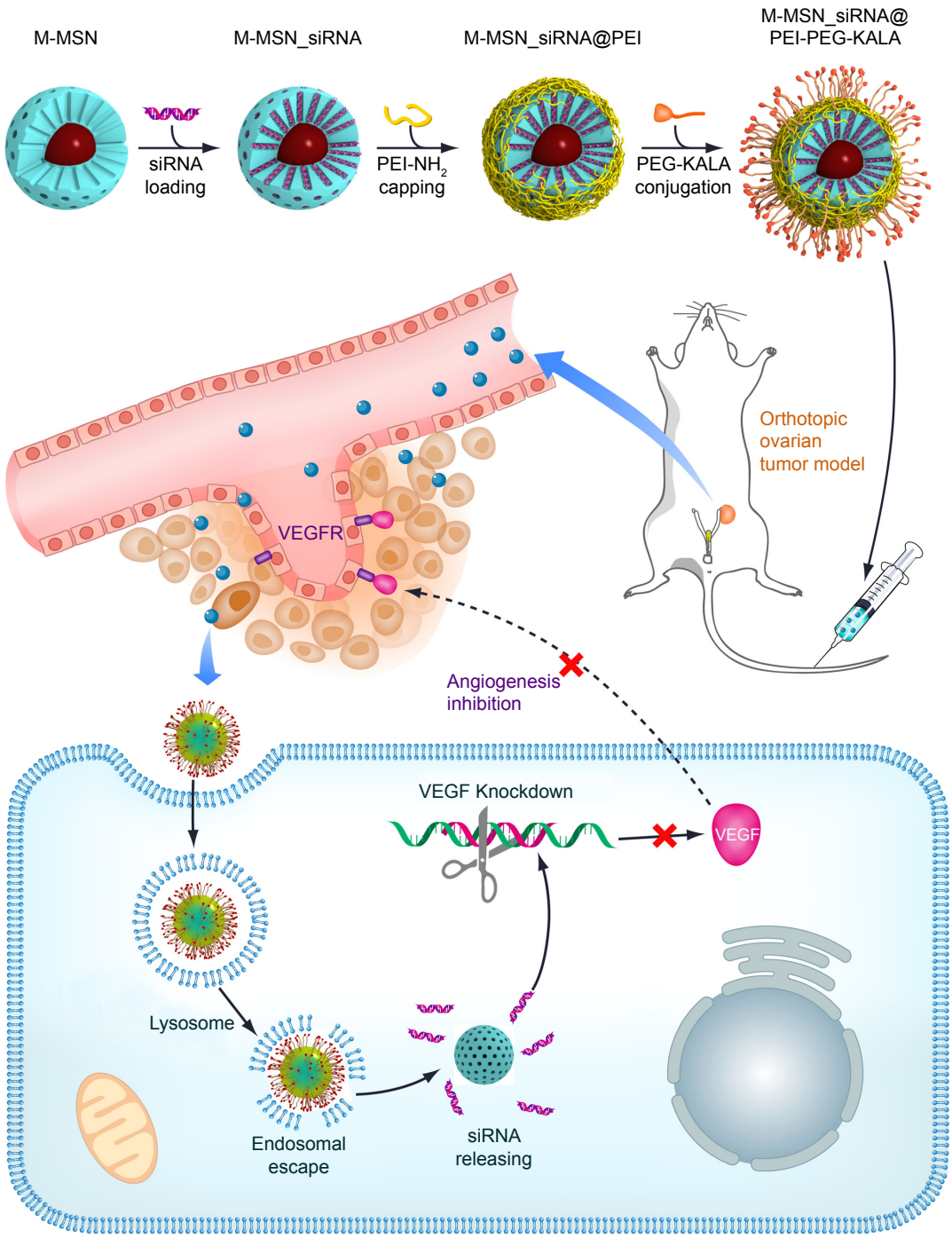

Figure 1 Schematic representation of the design of this study.
Note: Synthesis of M-MSN_siRNA@PEI-PEG-KALA (top) and systemic administration of VEGF siRNA via this nanocarrier into orthotopic ovarian tumor-bearing mice led to effective silencing of VEGF gene expression in cancer cells and inhibited angiogenesis, ultimately leading to suppression of cancer growth.
Abbreviations: M-MSN, magnetic mesoporous silica nanoparticle; siRNA, small interfering RNA; PDI, polydispersity index; PEI, polyethylenimine; PEG, polyethylene glycol; KALA, a type of fusogenic peptide; VEGF, vascular endothelial growth factor.

In brief, M-MSNs and siRNA molecules were mixed in a loading solution containing 0.67 M guanidine hydrochloride and 66.7% ethanol (v/v) for 1 hour. The free siRNA concentration in the supernatant was measured using a NanoDrop1000 after centrifugation at 10,625 *g*-force. The amount of siRNA loaded in the M-MSNs was regulated by increasing the concentration of siRNA without a volume change in the loading solution. The siRNA-encapsulated M-MSNs were then capped with PEI in ethanol solution via an electrostatic interaction to construct M-MSN_siRNA@PEI under ultrasonic conditions.

Next, 250 μL of NHS-PEG-Mal dissolved in dimethyl sulfoxide (8 mg/mL; PEG refers to this size thereafter)[24] containing maleimide moieties was made to react with the thiol groups in 50 μL of KALA[25,26] peptide (dissolved in water, 0.5 mg/mL) to form an NHS-PEG-KALA conjugate, which was then grafted onto the surface of the prepared M-MSN_siRNA@PEI (1 mg applied M-MSN) via the reaction between the amino groups and NHS. The obtained composites were then washed with deionized water three times to eliminate the unreacted reagents and then separated from the solution by centrifugation at 10,625 *g*-force. Finally, the resultant siRNA nanocarrier was denoted as M-MSN_siRNA@PEI-PEG-KALA, the physicochemical properties of which were then characterized.

Cell culture and measurement of cytotoxicity

Human ovarian adenocarcinoma (SKOV3) cells purchased from the Shanghai Institute for Biological Sciences (Shanghai, People's Republic of China), were grown in Roswell Park Memorial Institute 1640 medium containing 10% (v/v) heat-inactivated fetal bovine serum and 1% (v/v) penicillin-streptomycin (100 U/mL penicillin G and 100 mg/mL streptomycin) at 37°C in a 5% CO_2 atmosphere and at 95% relative humidity.

Viability of the SKOV3 cells was measured using the MTT assay. The SKOV3 cells were seeded at a density of 1×10^4 cells per well on 96-well plates, and the following experiments were conducted until they reached 80% confluence. After removing the culture medium, the fresh medium was supplemented with 10% fetal bovine serum and various concentrations (50–400 μg/mL) of M-MSN_NC siRNA@PEI and M-MSN_NC siRNA@PEI-PEG-KALA. A negative control group was treated with an equivalent volume of culture medium. The cells were coincubated with nanoparticles for 24 hours, with addition of 20 μL of MTT solution (5 mg/mL in phosphate-buffered saline) into each well and further cultured for 5 hours. At the end of the assay, the medium was removed, and 150 μL of dimethyl sulfoxide was added to dissolve the blue formazan crystal produced by the proliferating cells. Finally, the plate was incubated at 37°C for 30 minutes, and absorbance at 570 nm was measured using a Victor 3 microplate reader (PerkinElmer, Boston, MA, USA). The averaged absorbance values were normalized to the negative control.

Effectiveness of gene knockdown by M-MSN_VEGF siRNA@PEI-PEG-KALA vector

For knockdown of the VEGF gene, SKOV3 cells were plated into a 24-well culture plate at a density of 6×10^4 cells per well. After incubating at 37°C for 24 hours, the cells were treated with M-MSN_VEGF siRNA@PEI-PEG-KALA nanocarriers. After 24 hours of incubation, the growth medium in each well was replaced with fresh growth medium. After incubating for another 24 hours, the supernatant medium in each well was collected, and the amount of VEGF secreted from the cells was determined using an enzyme-linked immunosorbent assay (ELISA) according to the manufacturer's instructions. For the VEGF gene silencing experiments, the dose of siRNA in each well was 150 nM. Lipofectamine 2000 was used as the control.

Orthotopic ovarian cancer-bearing mouse model

Nude female BALB/c mice (aged 5–6 weeks, weighing 18–20 g) were purchased from the Shanghai Slac Laboratory Animal Co Ltd (Shanghai, People's Republic of China). All animal procedures were performed according to protocols approved by the Animal Care and Use Committee of Shanghai Jiao Tong University, School of Medicine. Subdermal tumor-bearing mice were established by subcutaneous inoculation of SKOV3 cells (2×10^6/100 μL) into the right flank region of the hind leg. When the average volume of the tumor xenograft reached approximately 100 mm^3, each mouse was anesthetized by intraperitoneal injection of ketamine 10 mL/kg, and the tumor tissue was collected. The purpose of the subdermal SKOV3 tumor xenograft was to construct an orthotopic SKOV3 ovarian cancer model. When collected, the tumors were carefully cut into small tumor pellets (about 1 mm^3) to establish the orthotopic ovarian cancer model.

After anesthesia and skin disinfection, an incision about 1.0 cm in length was made in the skin just lateral to the midline of the lower back, until the ovary was visible under the muscle layer. After removing the right ovary, a tiny hole was made under the microscope, and the resultant tumor pellet was sutured into the ovarian bursa. The ovary was put back in place, and if no bleeding was noted, the incision on the muscle layer and body wall was closed separately.[27,28] Magnetic resonance imaging was performed 6 weeks later. The antitumor efficiency experiments were not performed until 10 days after the operation.

Antitumor efficiency

The in vivo antitumor efficiency of M-MSN_VEGF siRNA@PEI-PEG-KALA was estimated in SKOV3 orthotopic tumor-bearing mice. The tumor-bearing mice (n=20) were randomly assigned to four groups to receive saline, M-MSN@PEI-PEG-KALA, M-MSN_NC siRNA@

PEI-PEG-KALA, or M-MSN_VEGF siRNA@PEI-PEG-KALA at a dose of 100 mg/kg containing 3.5 nmol siRNA dispersed in 200 μL of saline. The intravenous injection was given at days 10, 14, 18, 23, and 30 after orthotopic inoculation of the SKOV3 tumor pellets. Body weight was measured every 5 days during the treatment period. One week after the final injection, the cancer-bearing mice were euthanized to obtain sample tissues (heart, liver, spleen, lung, kidney, and tumor) for hematoxylin and eosin staining and immunostaining analysis. The tumor volumes were measured using a caliper and calculated according to the following formula: tumor volume (cm^3) = (tumor length × tumor width^2)/2.[27,29–31]

Immunohistochemistry analysis and determination of intratumoral VEGF content

Immunohistochemistry was performed using an avidin-biotin complex protocol on paraffin-embedded tissue to assess the mechanism of in vivo antitumor efficiency. The excised tumor tissues were fixed using 4% polyformaldehyde, embedded in paraffin, and cut into 5 mm thick slices. Sections were incubated with 10% goat serum (Maixin-Bio) for 30 minutes to block nonspecific binding, then incubated overnight at 4°C with the following primary antibodies: Ki67 antibody (1:100), CD31 antibody (1:100), and VEGF antibody (1:200). The slides were incubated with biotinylated secondary antibody. The immunoreaction was then visualized using diaminobenzidine chromogen (Maixin-Bio). Negative controls were incubated in blocking serum alone. Five images were captured for each slide, which were stained for CD31 and Ki67. The microvessel density (MVD) was determined by counting the quantity of microvessels in each image, and the average quantity of vessels was represented as the MVD value. The number of Ki67-positive cells was counted in each 200 field, and the average value for the percentage of Ki67-positive cells was obtained from these fields. The average density of VEGF was obtained using Image-Pro Plus version 6.0 software from Media Cybernetics Inc. (Rockville, MD, USA).

The excised tumor tissues were weighed and homogenized in a protein lysis solution (radio immunoprecipitation assay buffer supplemented with phenylmethanesulfonyl fluoride and a cocktail of protease inhibitors) using an electronic tissue homogenizer (Sonics & Materials Inc., Newton, CT, USA). The mixture was centrifuged for 10 minutes at 10,625 *g*-force (4°C), and the resultant supernatant was then analyzed using ELISA to detect the level of VEGF (quantikine human VEGF immunoassay kit, R&D Systems) following the manufacturer's instructions.

T_2-weighted magnetic resonance imaging

T_2-weighted imaging was performed using a MesoMR23-060H-I imaging instrument (Shanghai Niumag Corporation, Shanghai, People's Republic of China). The orthotopic ovarian cancer-bearing mice were anaesthetized with ketamine 10 mL/kg. Imaging was performed before and after the intravenous injection of M-MSN_NC siRNA@PEI-PEG-KALA at a dose of 100 mg/kg. The instrument parameters were set as follows: a 0.55 T magnet, K space 192 * 256 μm, section thickness 3 mm, echo time 60 msec, repetition time 2,000 msec, FOVRead 100 mm, FOVPhase 100 mm, and a total of four scans.

Statistical analysis

Statistical Package for the Social Sciences version 11.0 software (SPSS Inc., Chicago, IL, USA) was used for statistical analyses. The data are presented as the mean ± standard deviation and analyzed by one-way analysis of variance followed by the Student's *t*-test. Statistical significance was set at alpha values of $P<0.0001$ (very significant), $P<0.001$ (highly significant), and $P<0.01$ (significant).

Results and discussion

Characterization of M-MSN_siRNA@PEI-PEG-KALA

The morphology of M-MSN_siRNA@PEI-PEG-KALA was characterized by transmission electron microscopy (Figure 2A). Dynamic light scattering analysis showed that M-MSN_siRNA@PEI-PEG-KALA had a diameter of ~160 nm accompanied by a polydispersity index of 0.095 (Figure 2B) in saline, with a zeta potential of approximately +23 mV in water (Figure 2C), indicating that this nanocarrier was potentially suitable for cellular endocytosis.[32,33] Thermogravimetric analysis was then performed to determine the amount of modified molecules in the nanocarrier. The relative mass ratios of PEI and PEG in M-MSN_siRNA@PEI-PEG-KALA were ~14.6% and ~11.0%, respectively (Figure S1A). The grafted KALA in the nanocarrier was ~17.4% of the total applied KALA, which was captured using fluorescein isothiocyanate-labeled KALA (Figure S1B). Each M-MSN_siRNA@PEI-PEG-KALA nanocarrier had a superparamagnetic core, which rendered good linearity between the T_2 relaxation rate ($1/T_2$) and the iron concentration measured at 0.5 Tesla with a spin-echo pulse sequence, indicating M-MSN_siRNA@PEI-PEG-KALA as a contrast agent with an r_2 value of 226.92 $mM^{-1}s^{-1}$ (Figure 2D). In this work, the amount of siRNA loaded into the nanocarrier was ~30 mg siRNA/g M-MSNs (1.875 nmol/mg M-MSNs) and ~28 mg siRNA/g M-MSNs (1.75 nmol/mg M-MSNs) for in vitro gene silencing and in vivo cancer therapy, respectively.

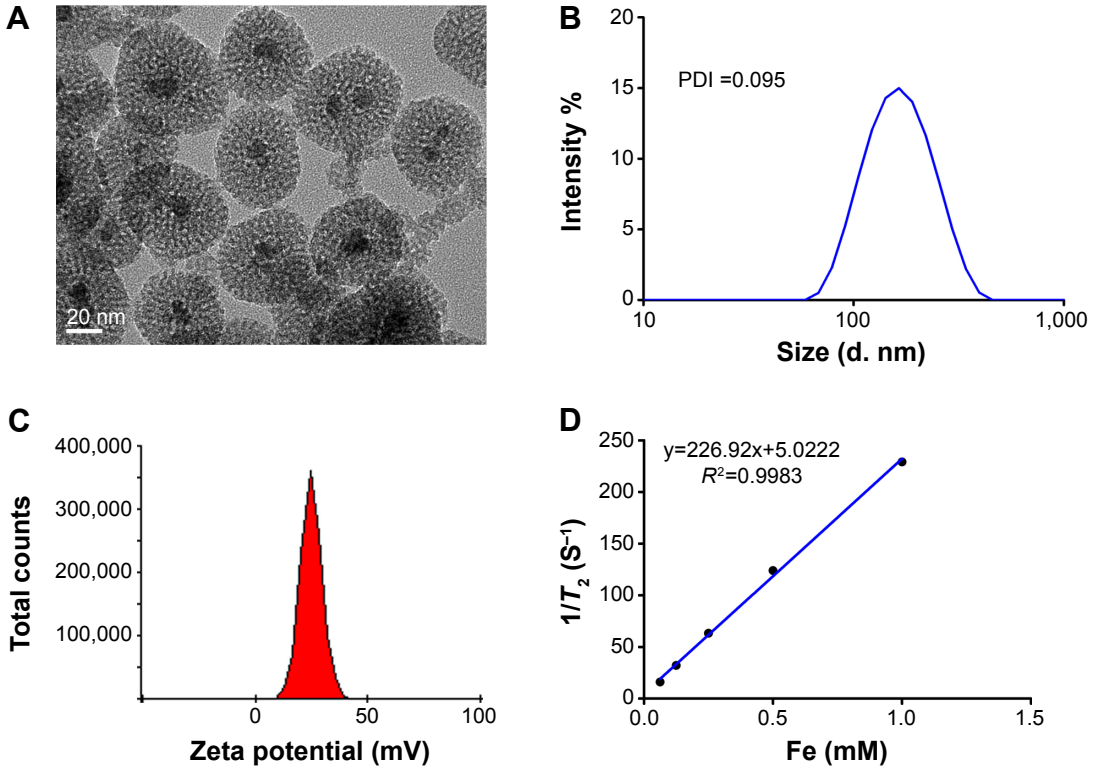

Figure 2 (**A**) Transmission electron microscopic image of M-MSN_siRNA@PEI-PEG-KALA. (**B**) Dynamic light scattering measurements of size distribution for M-MSN_ siRNA@PEI-PEG-KALA (dispersed in saline). (**C**) Zeta potential of M-MSN_siRNA@PEI-PEG-KALA. (**D**) T_2 relaxation rate ($1/T_2$) as a function of iron concentration for M-MSN_ siRNA@PEI-PEG-KALA.

Notes: Scale bar, 20 nm. (**B**) The polydispersity index (PDI) of this nanocarrier was 0.095.

Abbreviations: M-MSN, magnetic mesoporous silica nanoparticle; siRNA, small interfering RNA; PEI, polyethylenimine; PEG, polyethylene glycol; KALA, a type of fusogenic peptide.

Cytotoxicity and RNAi efficiency of M-MSN_siRNA@PEI-PEG-KALA

Cytotoxicity is a critical factor in the development of a novel molecular delivery system. Cytotoxicity was determined before applying M-MSN_siRNA@PEI-PEG-KALA to estimate the gene silencing efficacy. SKOV3 cells were incubated with M-MSN_NC siRNA@PEI-PEG-KALA at various concentrations for 24 hours. For comparison, M-MSN_NC siRNA@PEI, without the PEG-KALA modification, was introduced as a positive control. As shown in Figure 3A, M-MSN_NC siRNA@PEI-PEG-KALA showed negligible cytotoxicity even at a high dose (400 μg/mL, applied M-MSNs) when compared with M-MSN_NC siRNA@PEI (Figure S2), which showed severe cytotoxicity even at a lower concentration (100 μg/mL, applied M-MSNs). These results demonstrated that M-MSN_NC siRNA@PEI-PEG-KALA had good compatibility due to successful modification of PEG and could be considered more suitable for in vivo application.

VEGF is overexpressed and secreted by most tumor cells, especially in ovarian cancer, regulating the growth of new blood vessels and maintaining their survival during tumor growth.[4] Therefore, knockdown of VEGF gene expression has been widely used in antiangiogenesis therapy, and is always mediated by RNAi technology. In the current study, in vitro RNAi experiments demonstrated that VEGF gene knockdown regulated by M-MSN_VEGF siRNA@PEI-PEG-KALA vehicles (at a concentration of 80 μg/mL applied M-MSN containing 150 nM VEGF-siRNA, determined by an siRNA dosage test) was more effective than commercial Lipofectamine 2000 and the other four control groups in SKOV3 cells with an equivalent siRNA dosage, as shown in Figure 3B. VEGF expression in the untreated group was defined as 100%. Consequently, M-MSN_VEGF siRNA@PEI-PEG-KALA nanocarriers better inhibited VEGF expression, which fell to ~20%, compared with the Lipofectamine 2000 group, in which VEGF expression dropped to ~40%. This high gene silencing efficiency of M-MSN_VEGF siRNA@PEI-PEG-KALA is partly a result of modification with KALA, which not only promoted the internalization capability of the nanocarrier (Figures S3A and S4) but also mediated the timely escape of the nanocarrier from the lysosome (Figure S3B). The siRNA was then released from its vector into the cytoplasm (Figure S3C) to perform the RNAi function.

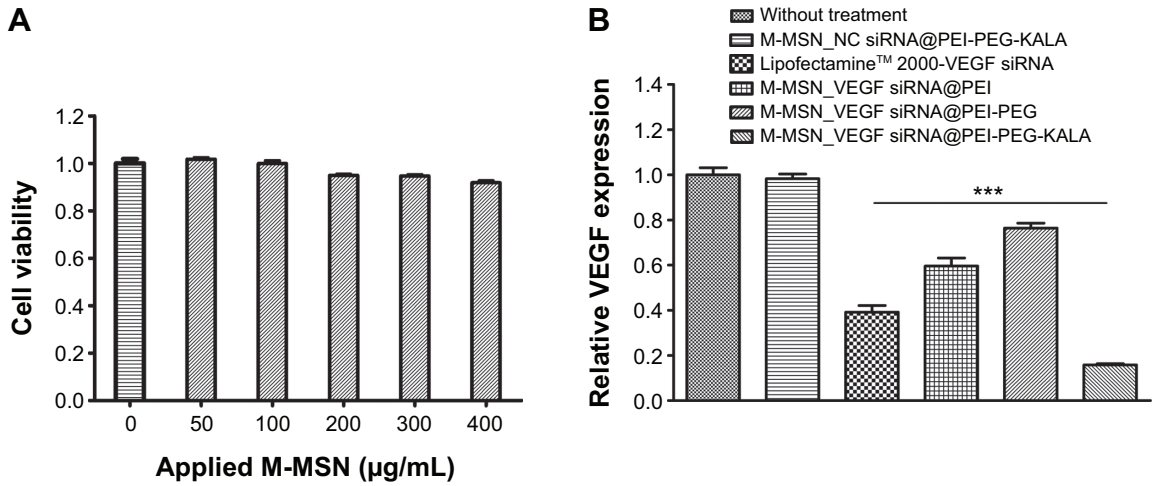

Figure 3 (**A**) An MTT assay was performed to evaluate the viability of the SKOV3 cells on exposure to M-MSN_NC siRNA@PEI-PEG-KALA containing various concentrations of M-MSNs, ranging from 50 to 400 μg/mL. (**B**) Downregulated vascular endothelial growth factor (VEGF) expression in SKOV3 cells by the M-MSN_VEGF siRNA@PEI-PEG-KALA, M-MSN_VEGF siRNA@PEI and M-MSN_VEGF siRNA@PEI-PEG delivery systems.

Notes: (**A**) 0 denotes absence of treatment. (**B**) The dose of siRNA(NCor VEGF) was 150 nM within 80 μg/mL of M-MSNs. An identical quantity of siRNA was also transfected with Lipofectamine™ 2000 (***$P<0.0001$, n=3).

Abbreviations: MTT, 3-(4,5-dimethylthiazol-2-yl)-2,5-diphenyltetrazolium bromide; M-MSN, magnetic mesoporous silica nanoparticle; PEI, polyethylenimine; PEG, polyethylene glycol; KALA, a type of fusogenic peptide; VEGF siRNA, vascular endothelial growth factor small interfering RNA; NC siRNA, negative control small interfering RNA.

Probing ovarian cancer in vivo

Although the long-term outcomes for patients with stage III or IV ovarian cancer are poor, the 5-year overall survival of stage I patients can reach 90%. This has led researchers to develop and test methods to detect ovarian cancer at an early stage, which would likely have a significant impact on mortality rates.[34] Thus, progress in high-quality ovarian cancer imaging might be a promising way to diagnose this cancer at an early stage. M-MSN_siRNA@PEI-PEG-KALA was created with a core of superparamagnetic nanoparticles that proved to be an excellent magnetic resonance contrast agent due to their decreased transverse relaxation time (T_2) with increased iron concentration, which was measured at 0.5 T with a spin-echo pulse sequence, as shown in Figure 2D. Whether systemically injected nanoparticles reach the tumor site and accumulate readily is critical for cancer therapy and visualized via a clinically relevant imaging paradigm. Twenty-four hours after intravenous administration of the M-MSN_siRNA@PEI-PEG-KALA vector, significant signal reduction (darkness) was observed around the periphery of the tumor site (the red circle region) in our orthotopic ovarian cancer model compared with the signal before injection (Figure 4). This phenomenon of nanocarrier distribution in tumor is explained due to the rare neovasculature in tumor center with high extravasation ability, overall leading to limited nanoparticles distribution in the inner necrotic zone.[35,36] Accumulation of the nanocarrier in the tumor region was also confirmed by detection of iron levels using Prussian blue staining, as shown in Figure S5. The magnetic resonance imaging results suggest that M-MSN_siRNA@PEI-PEG-KALA as a highly effective T_2-weighted contrast agent is suitable for widespread application and could facilitate research on the optimal dosage and therapeutic window through the various dark areas in the tumor region.

Antitumor efficiency and systemic toxicity in vivo

On observing that the M-MSN_VEGF siRNA@PEI-PEG-KALA delivery system achieved highly effective VEGF gene knockdown in SKOV3 cells, we then investigated whether this vector could inhibit tumor growth in vivo. Orthotopic ovarian tumor-bearing mice were created to evaluate the antitumor efficacy of M-MSN_VEGF siRNA@PEI-PEG-KALA via inoculation of SKOV3 tumor pellets into female nude mice, as described earlier. Ten days after inoculation, the mice were treated with various vectors, including VEGF-siRNA, NC-siRNA, an empty vector, or saline, for a total of five intravenous injections. Each injection contained a 100 mg/kg (applied M-MSNs) dose with or without 3.5 nmol siRNA. The results showed profound tumor suppression in the group treated with M-MSN_VEGF siRNA@PEI-PEG-KALA, with markedly delayed tumor growth (115.4±37.35 mm^3, n=5). In contrast, tumor volumes grew rapidly in the saline group to a mean of 704.4±108.7 mm^3 (n=5). Tumor volumes in the groups treated with M-MSN@PEI-PEG-KALA and

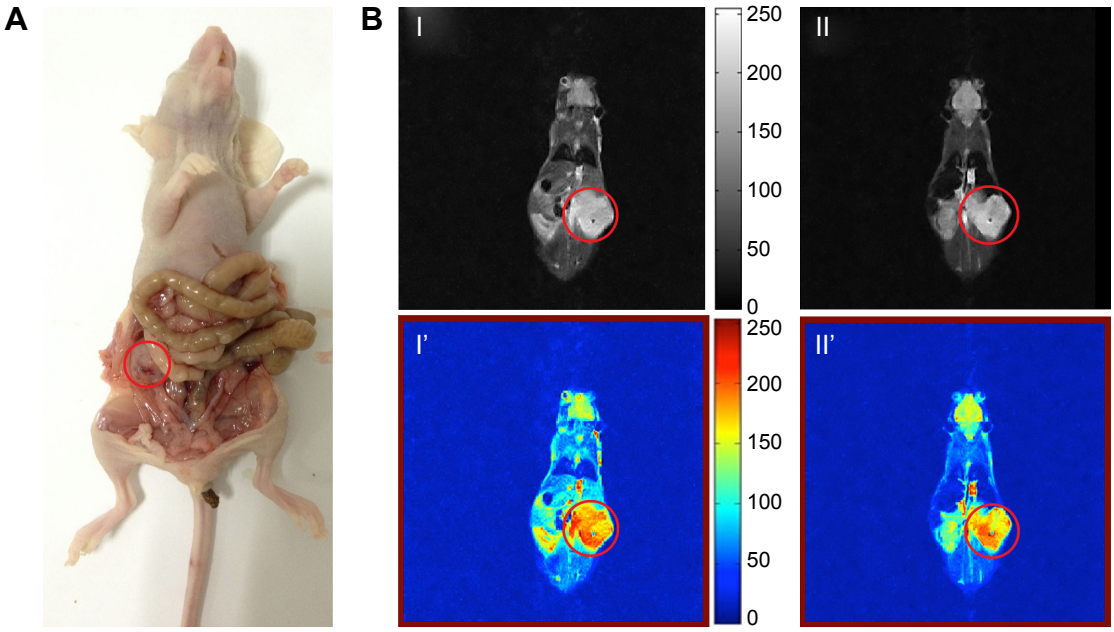

Figure 4 (**A**) Orthotopic ovarian mouse tumor (red circle is the tumor position). (**B**) In vivo T_2-weighted magnetic resonance images of the xenograft tumor model before (left) and 24 hours after (right) injection of M-MSN_NC siRNA@PEI-PEG-KALA.
Notes: Gray-scale images (top, I and II) and pseudocolor images (bottom, I' and II') are shown.
Abbreviations: M-MSN, magnetic mesoporous silica nanoparticles; PEI, polyethylenimine; PEG, polyethylene glycol; KALA, a type of fusogenic peptide; NC siRNA, negative control small interfering RNA.

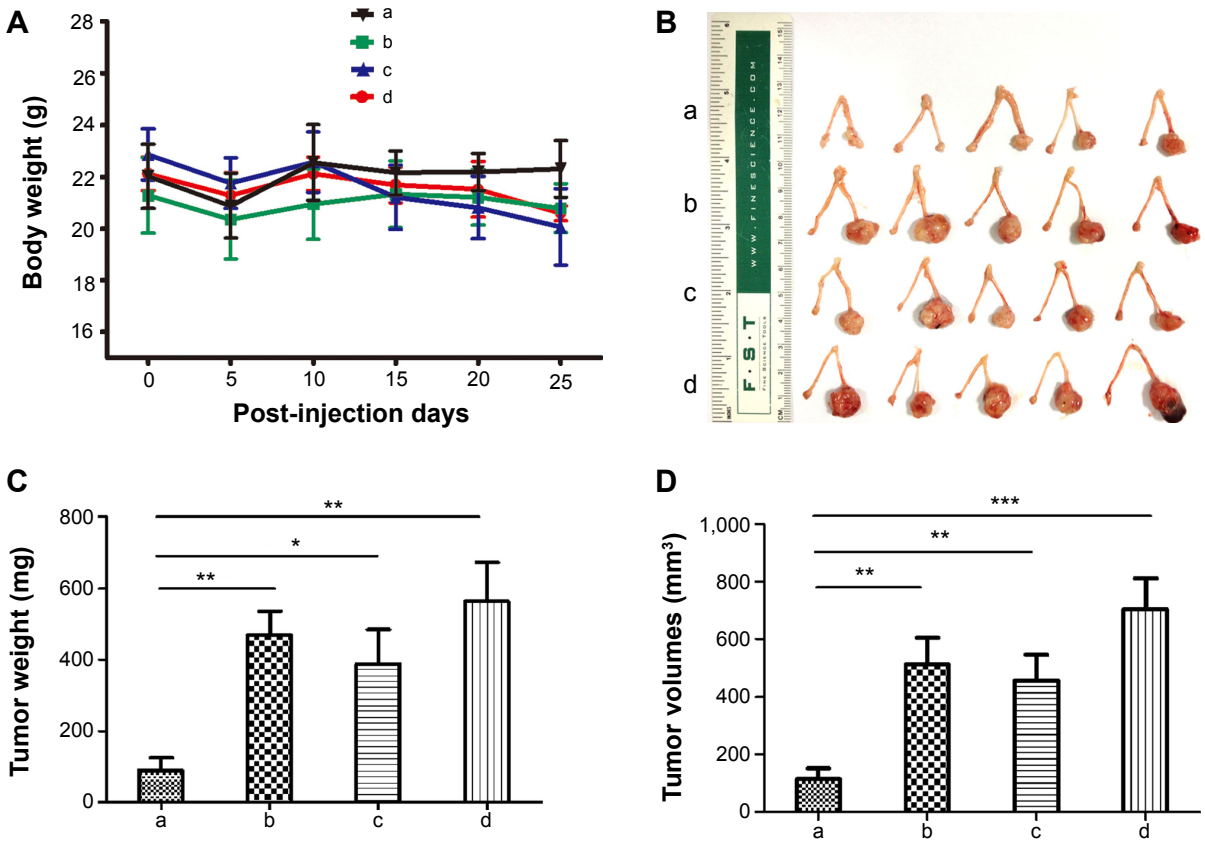

Figure 5 (**A**) Changes in body weight in the different treatment groups. (**B**) Tumors collected from the four treatment groups at the end of the experiment. Tumor weights (**C**) and tumor volumes (**D**) were measured after euthanizing the mice.
Notes: Data represent the mean ± standard deviation. (*P<0.01; **P<0.001; ***P<0.0001; n=5). a: M-MSN_VEGF siRNA@PEI-PEG-KALA; b: M-MSN_NC siRNA@PEI-PEG-KALA; c: M-MSN@PEI-PEG-KALA; d: saline.
Abbreviations: M-MSN, magnetic mesoporous silica nanoparticles; PEI, polyethylenimine; PEG, polyethylene glycol; KALA, a type of fusogenic peptide; NC siRNA, negative control small interfering RNA; VEGF siRNA, vascular endothelial growth factor small interfering RNA.

M-MSN_NC siRNA@PEI-PEG-KALA reached means of 457.3±89.42 mm^3 and 513.7±91.8 mm^3 (n=5), respectively (Figure 5B and D). The same inhibitory effect was also reflected in tumor weight (Figure 5C). The average tumor weight in the M-MSN_VEGF siRNA@PEI-PEG-KALA group was 89.60±35.95 mg (n=5), which was significantly lower than the mean tumor weight of 468.8±67.98 mg (n=5) in the M-MSN_NC siRNA@PEI-PEG-KALA group, 389.0±96.73 mg (n=5) in the M-MSN@PEI-PEG-KALA group, and 564.2±107.9 mg (n=5) in the saline group. Meanwhile, all mice maintained a steady body weight, with few changes over time (Figure 5A), indicating that the nanocarrier was generally safe and biocompatible, as demonstrated previously.

The collective results show that the nanocarrier used in the present study achieved highly effective tumor inhibition in vivo, which was largely attributable to the design and optimization of the particles, and especially the PEGylation modification, which improved the monodispersity in saline, reduced absorption and adhesion by the reticuloendothelial system, and resulted in better accumulation in the tumor region.

The corresponding biodistribution study of M-MSN_siRNA@PEI-PEG-KALA in the major organs was reported in our previous work,[21] which showed that the highest concentration of iron (on behalf of the nanocarrier, because each nanocarrier has a superparamagnetic Fe_4O_3 core) was found in the liver (~27%), followed by the lung (~15%), spleen (~14%), and kidney (~4%), as tested by atomic absorption analysis 1 day after injection. The nanocarrier was readily removed from these tissues, as all iron content decreased over time (3 days and 7 days after injection). Consequently, VEGF gene knockdown resulted in inhibition of angiogenesis, which reduced or even halted tumor growth. The safety and biocompatibility of systemic application of M-MSN_VEGF siRNA@PEI-PEG-KALA, after five repeated injections and following the therapeutic regime, was determined by assessment of markers indicating nephrotoxicity and hepatotoxicity (Figure S6) and corroborated by hematoxylin and eosin staining (Figure S7) for the main organs (heart, liver, spleen, lungs, and kidneys). Overall, the results indicate that the nanocarrier has negligible side effects and is an effective and a safe carrier for delivery of siRNA in the treatment of ovarian cancer.

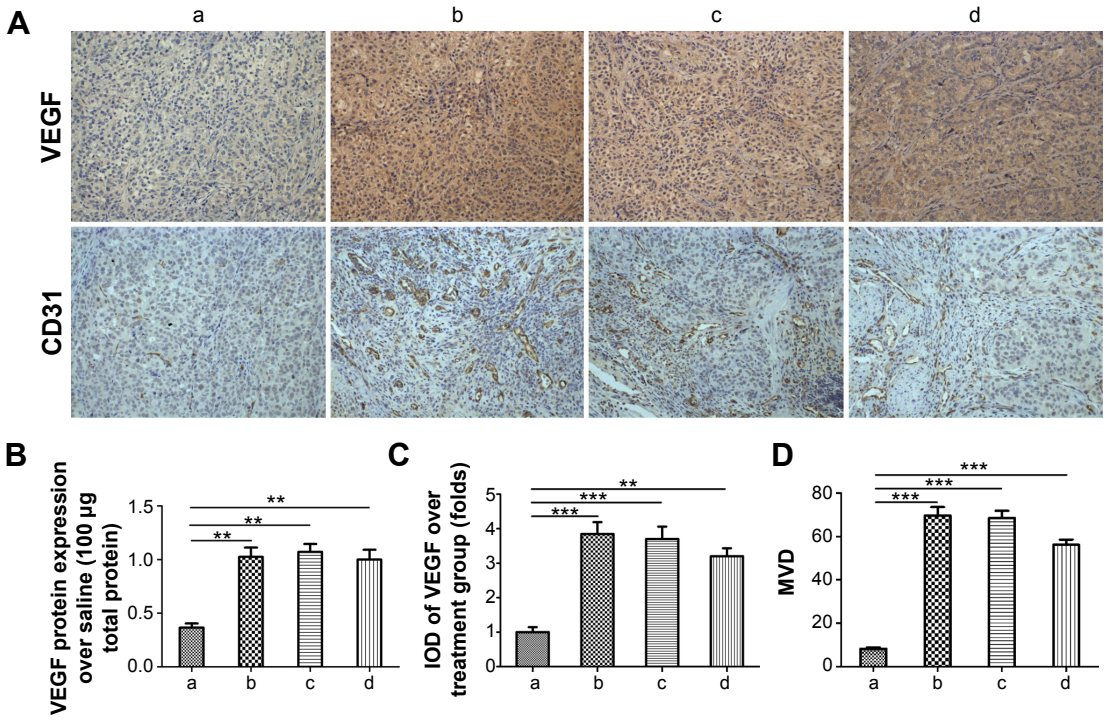

Figure 6 (**A**) Immunohistological analysis for VEGF expression in intratumoral sections (top) and microvessel density represented by CD31-positive endothelial cells (bottom) in the four treatment groups. (**B**) Intratumoral VEGF expression was measured by enzyme-linked immunosorbent assay. Statistical data reflect VEGF (**C**) and CD31 (**D**) expression in tumoral sections, respectively.

Notes: Data represent the mean ± standard deviation. (**$P<0.001$; ***$P<0.0001$; n=5). Magnification, 20×. a: M-MSN_VEGF siRNA@PEI-PEG-KALA; b: M-MSN_NC siRNA@PEI-PEG-KALA; c: M-MSN@PEI-PEG-KALA; d: saline.

Abbreviations: IOD, integral optical density; VEGF, vascular endothelial growth factor; M-MSN, magnetic mesoporous silica nanoparticle; MVD, microvessel density; PEI, polyethylenimine; PEG, polyethylene glycol; KALA, a type of fusogenic peptide.

Quantification of intratumoral VEGF content and immunohistochemistry

The collected tumor tissues were analyzed further for intratumoral VEGF levels and MVD. As shown in Figure 6B, the average VEGF protein expression level measured by ELISA assay was inhibited by ~65% after treatment with M-MSN_VEGF siRNA@PEI-PEG-KALA, which showed more significant knockdown efficacy than that found for the three untreated groups. Correspondingly, intratumoral VEGF and MVD were determined by immunohistochemistry analysis, represented by images of labeled VEGF proteins and CD 31-positive microvascular endothelial cells, respectively (Figure 6A). The statistical data (showing ~75% inhibition) from multiple tumor sections are shown in Figure 6C and D. Meanwhile, Ki67 expression was measured in tumor sections, and was associated with cell proliferation that was probably influenced by various VEGF levels. Treatment with M-MSN_VEGF siRNA@PEI-PEG-KALA resulted in less Ki67 expression than in the other three control groups (Figure S8). Interestingly, the decreased Ki67-positive signals as compared with the greater reduction in VEGF content and MVD as well as discrepancy in weights/volumes in tumors were observed. These results indicate that strong inhibition of tumor growth resulted from VEGF gene knockdown by M-MSN_VEGF siRNA@PEI-PEG-KALA (as shown by a decreased number of CD31-positive endothelial cells), slower cell proliferation (represented by Ki67 levels), or other biological mechanisms that would be considered in future investigations. Essentially, M-MSN_VEGF siRNA@PEI-PEG-KALA significantly suppressed expression of the VEGF gene, inhibited angiogenesis effectively, and cut off the supply of oxygen and nutrients, which finally inhibited tumor growth.

Conclusion

In this study, VEGF gene expression was effectively inhibited by systemic administration of VEGF siRNA via an M-MSN_siRNA@PEI-PEG-KALA nanocarrier, which resulted in significant suppression of orthotopic ovarian tumor growth due to markedly decreased angiogenesis, and without systemic toxicity. In conclusion, the therapeutic effects shown in this study, which strongly inhibited orthotopic ovarian cancer, offer the potential for even broader therapeutic application of the M-MSN-based siRNA delivery system, which indeed showed high efficacy and biocompatibility when used in the treatment of lung cancer in our previous work. Moreover, in vivo magnetic resonance imaging confirmed the accumulation of nanoparticles in orthotopic ovarian tumor tissues via various darkness signals, and provided an efficient noninvasive imaging method for assessing siRNA delivery and antitumor effects. Finally, this versatile delivery system may have potential for clinical application in the treatment of ovarian cancer.

Acknowledgments

This work was supported by the National Science Foundation (81472426), the Physical Therapy for Ovarian Cancer Project from the Science and Technology Commission of Shanghai (11DZ2211002), grants from the State Key Laboratory of Oncogenes and Related Genes (91-14-03), the High Tech Program of MOST China (2013AA032203), and the Shanghai Health Bureau Key Disciplines and Specialties Foundation.

Disclosure

The authors report no conflicts of interest in this work.

References

1. Jelovac D, Armstrong DK. Recent progress in the diagnosis and treatment of ovarian cancer. *CA Cancer J Clin*. 2011;61(3):183–203.
2. Vaughan S, Coward JI, Bast RC Jr, et al. Rethinking ovarian cancer: recommendations for improving outcomes. *Nat Rev Cancer*. 2011;11(10):719–725.
3. Carmeliet P, Jain RK. Angiogenesis in cancer and other disease. *Nature*. 2000;407(6801):249–257.
4. Gavalas NG, Liontos M, Trachana S-P, et al. Angiogenesis-related pathways in the pathogenesis of ovarian cancer. *Int J Mol Sci*. 2013;14(8):15885–15909.
5. Potente M, Gerhardt H, Carmeliet P. Basic and therapeutic aspects of angiogenesis. *Cell*. 2011;146(6):873–887.
6. Welti J, Loges S, Dimmeler S, Carmeliet P. Recent molecular discoveries in angiogenesis and antiangiogenic therapies in cancer. *J Clin Invest*. 2013;123(8):3190–3200.
7. Krämer I, Lipp HP. Bevacizumab, a humanized anti-angiogenic monoclonal antibody for the treatment of colorectal cancer. *J Clin Pharm Ther*. 2007;(32):1–14.
8. Gordon CR, Rojavin Y, Patel M, et al. A review on bevacizumab and surgical wound healing: an important warning to all surgeons. *Ann Plast Surg*. 2009;62(6):707–709.
9. Eskander RN, Tewari KS. Incorporation of anti-angiogenesis therapy in the management of advanced ovarian carcinoma – mechanistics, review of phase III randomized clinical trials, and regulatory implications. *Gynecol Oncol*. 2014;132(2):496–505.
10. Okines A, Cunningham D. Current perspective: bevacizumab in colorectal cancer – a time for reappraisal? *Eur J Cancer*. 2009;45(14):2452–2461.
11. Pavlidis ET, Pavlidis TE. Role of bevacizumab in colorectal cancer growth and its adverse effects: a review. *World J Gastroenterol*. 2013;19(31):5051–5060.
12. Liu F, Gao G, Tu K, Yu L, Gao J. Small interfering RNA targeting MDR1 inhibits ovarian cancer growth and increases efficacy of chemotherapy in vivo. *Chin J Cancer Res*. 2009;21(4):318–324.
13. Fan Y, Xin XY, Chen BL, Ma X. Knockdown of Rab25 expression by RNAi inhibits growth of human epithelial ovarian cancer cells in vitro and in vivo. *Pathology*. 2006;38(6):561–567.
14. Shah V, Taratula O, Garbuzenko OB, Taratula OR, Rodriguez-Rodriguez L, Minko T. Targeted nanomedicine for suppression of CD44 and simultaneous cell death induction in ovarian cancer: an optimal delivery of siRNA and anticancer drug. *Clin Cancer Res*. 2013;19(22):6193–6204.

15. Koyanagi T, Suzuki Y, Saga Y, et al. In vivo delivery of siRNA targeting vasohibin-2 decreases tumor angiogenesis and suppresses tumor growth in ovarian cancer. *Cancer Sci*. 2013;104(12):1705–1710.
16. Goldberg MS. siRNA delivery for the treatment of ovarian cancer. *Methods*. 2013;63(2):95–100.
17. Florinas S, Kim J, Nam K, Janát-Amsbury MM, Kim SW. Ultrasound-assisted siRNA delivery via arginine-grafted bioreducible polymer and microbubbles targeting VEGF for ovarian cancer treatment. *J Control Release*. 2014;183:1–8.
18. Lai C-Y, Trewyn BG, Jeftinija DM, et al. A mesoporous silica nanosphere-based carrier system with chemically removable CdS nanoparticle caps for stimuli-responsive controlled release of neurotransmitters and drug molecules. *J Am Chem Soc*. 2003;125(15):4451–4459.
19. Yang P, Gai S, Lin J. Functionalized mesoporous silica materials for controlled drug delivery. *Chem Soc Rev*. 2012;41(9):3679–3698.
20. Miele E, Spinelli GP, Miele E, et al. Nanoparticle-based delivery of small interfering RNA: challenges for cancer therapy. *Int J Nanomedicine*. 2012;7:3637–3657.
21. Chen Y, Gu H, Zhang DS-Z, Li F, Liu T, Xia W. Highly effective inhibition of lung cancer growth and metastasis by systemic delivery of siRNA via multimodal mesoporous silica-based nanocarrier. *Biomaterials*. 2014;35(38):10058–10069.
22. Li X, Zhang J, Gu H. Adsorption and desorption behaviors of DNA with magnetic mesoporous silica nanoparticles. *Langmuir*. 2011;27(10):6099–6106.
23. Li X, Xie QR, Zhang J, Xia W, Gu H. The packaging of siRNA within the mesoporous structure of silica nanoparticles. *Biomaterials*. 2011;32(35):9546–9556.
24. Yang X, Du J, Dou S, Mao C, Long H, Wang J. Sheddable ternary nanoparticles for tumor acidity-targeted siRNA delivery. *ACS Nano*. 2012;6(1):771–781.
25. Lee H, Jeong JH, Park TG. PEG grafted polylysine with fusogenic peptide for gene delivery: high transfection efficiency with low cytotoxicity. *J Control Release*. 2002;79(1–3):283–291.
26. Min S-H, Kim DM, Kim MN, et al. Gene delivery using a derivative of the protein transduction domain peptide, K-Antp. *Biomaterials*. 2010;31(7):1858–1864.
27. Wang Y, Liu P, Qiu L, et al. Toxicity and therapy of cisplatin-loaded EGF modified mPEG-PLGA-PLL nanoparticles for SKOV3 cancer in mice. *Biomaterials*. 2013;34(16):4068–4077.
28. Wang Y, Liu P, Duan Y, et al. Specific cell targeting with APRPG conjugated PEG-PLGA nanoparticles for treating ovarian cancer. *Biomaterials*. 2014;35(3):983–992.
29. Li X, Chen Y, Wang M, Ma Y, Xia W, Gu H. A mesoporous silica nanoparticle-PEI-fusogenic peptide system for siRNA delivery in cancer therapy. *Biomaterials*. 2013;34(4):1391–1401.
30. Huang H-Y, Kuo W-T, Chou M-J, Huang Y-Y. Co-delivery of anti-vascular endothelial growth factor siRNA and doxorubicin by multi-functional polymeric micelle for tumor growth suppression. *J Biomed Mater Res A*. 2011;97(3):330–338.
31. Han L, Huang R, Li J, Liu S, Huang S, Jiang C. Plasmid pORF-hTRAIL and doxorubicin co-delivery targeting to tumor using peptide-conjugated polyamidoamine dendrimer. *Biomaterials*. 2011;32(4):1242–1252.
32. Win KY, Feng S-S. Effects of particle size and surface coating on cellular uptake of polymeric nanoparticles for oral delivery of anticancer drugs. *Biomaterials*. 2005;26(15):2713–2722.
33. Slowing II, Vivero-Escoto JL, Wu C-W, Lin VS-Y. Mesoporous silica nanoparticles as controlled release drug delivery and gene transfection carriers. *Adv Drug Deliv Rev*. 2008;60(11):1278–1288.
34. Cohen JG, White M, Cruz A, Farias-Eisner R. In 2014, can we do better than CA125 in the early detection of ovarian cancer? *World J Biol Chem*. 2014;5(3):286–300.
35. Bellomo C. A mathematical model of the immersion of a spherical tumor with a necrotic core into a nutrient bath. *Math Comput Model*. 2006;43(7–8):779–786.
36. Tindall MJ, Please CP, Peddie MJ. Modelling the formation of necrotic regions in avascular tumours. *Math Biosci*. 2008;211(1):34–55.

Supplementary materials

Materials and methods

Preparation of various M-MSNs

Magnetic mesoporous silica nanoparticles (M-MSNs) with a mean particle size of ~50 nm and a mean pore size of ~3.7 nm were prepared using the liquid-phase seeded growth approach[26] as previously reported.[27] Uniform Fe_3O_4 nanocrystals were synthesized using a modified coprecipitation method before being transferred into an aqueous phase with the assistance of the cationic surfactant, cetyltrimethylammonium bromide (CTAB). Propagation of the mesoporous silica shell was then performed by self-assembly of the CTAB and tetraethyl orthosilicate (TEOS) in basic solution. Finally, the template was removed by a highly efficient ion-exchange method using acetone as the precipitant and ethanol as a washing solvent. The resultant M-MSNs were collected by centrifugation and redispersed in ethanol at a concentration of ~5 mg/mL.

To synthesize cyanine 5.5-modified M-MSNs, 3 μL of 3-aminopropyltriethoxysilane (APTES) was added into the heated mixture of CTAB and TEOS, followed by heating at 70°C for 10 minutes while stirring. After the template removal steps were performed, as described above, 1 μg of cyanine 5.5-N-hydroxysuccinimide ester was reacted with 10 mg of M-MSNs (molar ratio of cyanine 5.5: APTES 1:1,000) in 10 mL of ethanol and stirred in darkness for 1 hour. The following template-removal and washing steps for cyanine 5.5-M-MSNs were the same as those mentioned above.

Intracellular localization of delivery vehicles

For the cell uptake study, SKOV3 cells were seeded into glass-bottom dishes at a density of 2×10^4 cells per dish and incubated at 37°C for 24 hours. The growth medium was then replaced with fresh medium containing M-MSN_FAM-NC siRNA@PEI-PEG-KALA (siRNA modified with fluorescein amidite) nanocarriers. Before imaging, cells were fixed by treatment with 4% paraformaldehyde and then stained with 4,6-diamidino-2-phenylindole. Confocal laser scanning microscopy (SP5 II; Leica, Wetzler, Germany) was used to assess the intracellular distribution of small interfering RNA (siRNA).

To confirm whether siRNA could pass through the endosomal barrier, the experiments were performed by complexing the SKOV3 cells with the M-MSN_FAM-NC siRNA@PEI-PEG-KALA vehicles for 36 hours. The SKOV3 cells were then treated with LysoTracker® Red DND for lysosome staining. Finally, the distribution of siRNA and lysosomes in the cytoplasm was characterized using confocal laser scanning microscope.

To investigate whether siRNA could be released from the nanocarriers at the 36-hour time point, a novel nanocarrier was constructed, which was composed of cyanine 5.5-modified M-MSNs and FAM-siRNA within the pores. The distribution of siRNA and M-MSNs in the cytoplasm was also determined using confocal laser scanning microscope.

Measurement of systemic toxicity

Measurements of markers for major nephrotoxicity and hepatotoxicity were performed on whole blood, and various biochemistry parameters were tested using the Diagnostic Auto-Biochemical Analyzer 7060 (Hitachi, Tokyo, Japan). The control group received saline without nanocarrier treatments using exactly the same regimen. All blood samples were stabilized with heparin (10 U/500 μL whole blood). For hematoxylin and eosin staining, major organs, including the heart, liver, spleen, lungs, and kidneys, were collected and fixed in 4% paraformaldehyde. Histological sections (10 μm thick) were created using a freezing microtome, stained with hematoxylin and eosin, and examined with a digital microscope (Leica).

Prussian blue staining

The tumor-bearing mice were euthanized to obtain the tumor tissue. A freezing microtome (CM1850; Leica) was used to cut the tumor into 6 μm thick slices. For Prussian blue staining, the slides were fixed with paraformaldehyde (4%) for 10 minutes, stained with 10 wt% potassium ferrocyanide for 10 minutes, and then stained with a mixture of 10% w/w Prussian blue and 20% HCl (1:1) for a further 30 minutes. After washing with water, the slides were counterstained with nuclear fast red for 15 minutes. The stained slides were dehydrated with graded levels of ethanol (70%, 95%, and 100%), and 100% xylene was then sequentially mixed with the samples for 5 minutes to complete dehydration. Finally, photographs were taken using a light microscope.

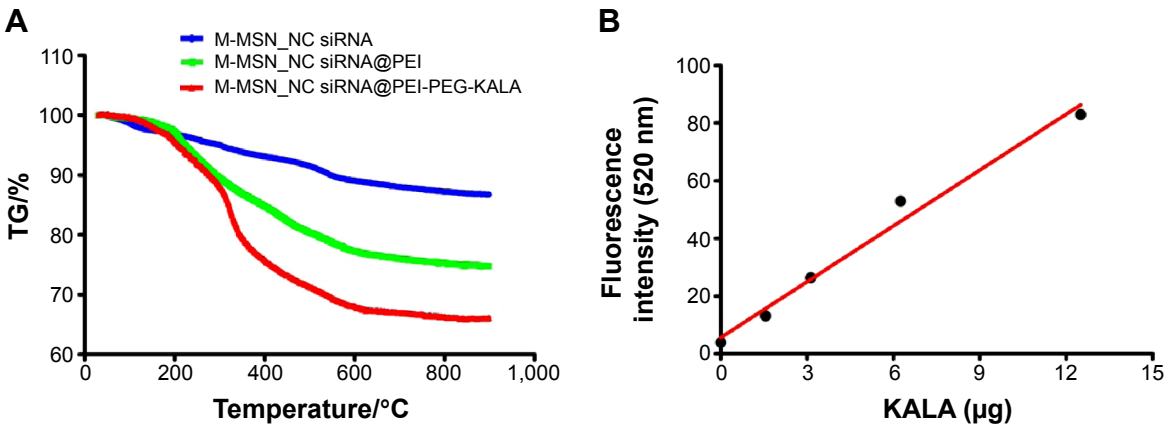

Figure S1 (**A**) TGA curves for various types of M-MSNs loaded with siRNA. (**B**) The standard curve for FITC-labeled KALA. Fluorescence intensity values at 520 nm versus the amount of FITC-labeled KALA.
Note: A linear fit was used for these data.
Abbreviations: TGA, thermogravimetric analysis; M-MSNs, magnetic mesoporous silica nanoparticles; FITC, fluorescein isothiocyanate; NC, negative control; PEI, polyethylenimine; PEG, polyethylene glycol; siRNA, small interfering RNA; KALA, a type of fusogenic peptide; TG, thermogravimetry.

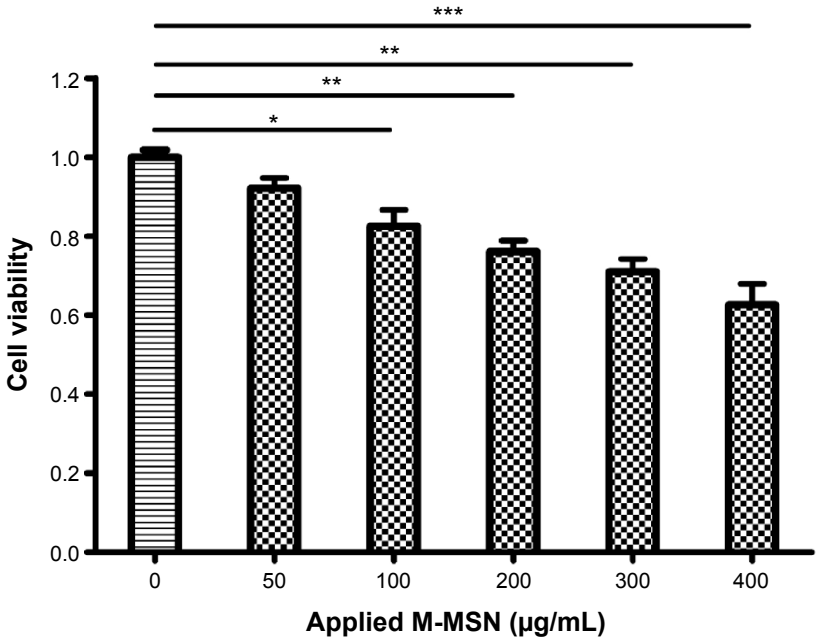

Figure S2 An MTT assay was performed to evaluate the viability of the SKOV3 cells by M-MSN_NC siRNA@PEI with various concentrations of applied M-MSNs ranging from 50 to 400 μg/mL.
Notes: 0 denotes absence of treatment. *$P<0.01$; **$P<0.001$; ***$P<0.0001$, n=3.
Abbreviations: MTT, 3-(4,5-dimethylthiazol-2-yl)-2,5-diphenyltetrazolium bromide; M-MSN, magnetic mesoporous silica nanoparticle; PEI, polyethylenimine; NC siRNA, negative control small interfering RNA.

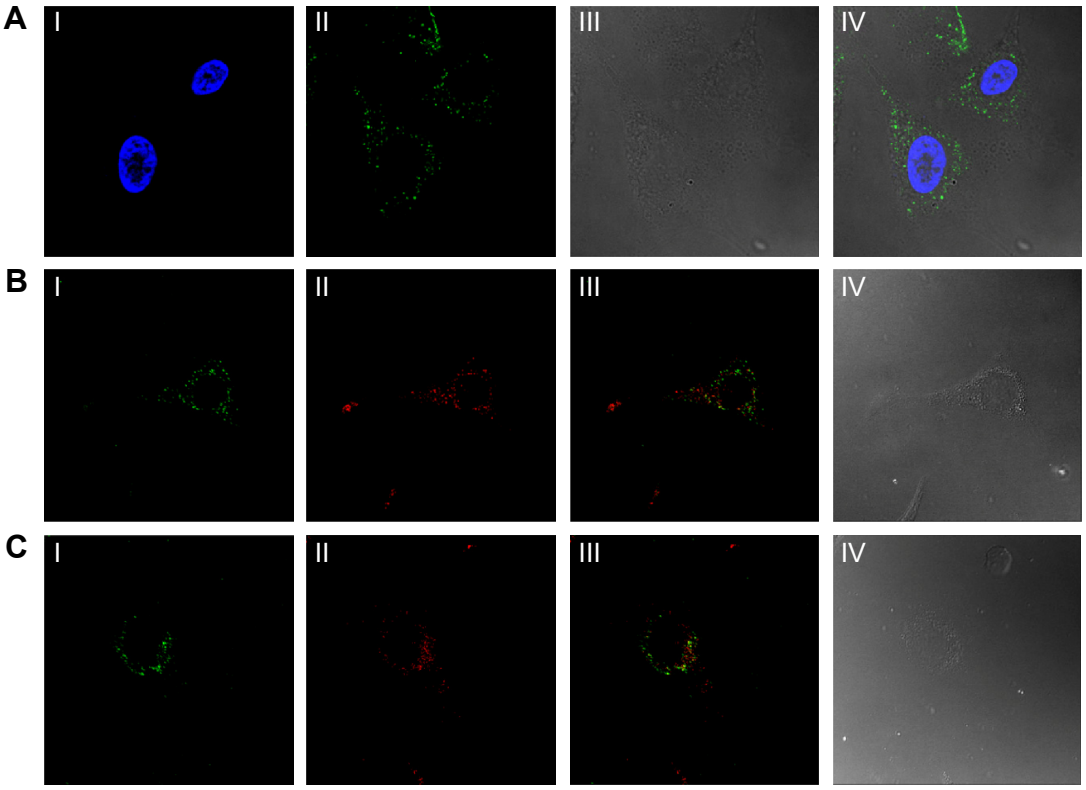

Figure S3 Fluorescent confocal laser scanning microscopic images of SKOV3 cells after incubation with M-MSN_NC siRNA@PEI-PEG-KALA nanocarriers for 24 hours (**A**, **B**) or 36 hours (**C**).

Notes: (AI) Blue fluorescent image of cell nucleus stained by DAPI, (AII) green fluorescent image of siRNA labeled by FAM, (AIII) differential interference contrast image, and (AIV) overlaying image of I–III. (BI) Green fluorescent images of FAM-labeled siRNA, (BII) red fluorescent images of endolysosomes stained by LysoTracker® Red DND, (BIII) merged image of I and II, and (BIV) differential interference contrast image. (CI) Green fluorescent images of FAM-labeled siRNA, (CII) red fluorescent images of M-MSNs labeled by cyanine 5.5, (CIII) merged image of I and II, and (CIV) differential interference contrast image. Magnification 20×.

Abbreviations: DAPI, 4′,6-diamidino-2-phenylindole; FAM, fluorescein amidite; M-MSN, magnetic mesoporous silica nanoparticle; PEI, polyethylenimine; PEG, polyethylene glycol; KALA, a type of fusogenic peptide; siRNA, small interfering RNA.

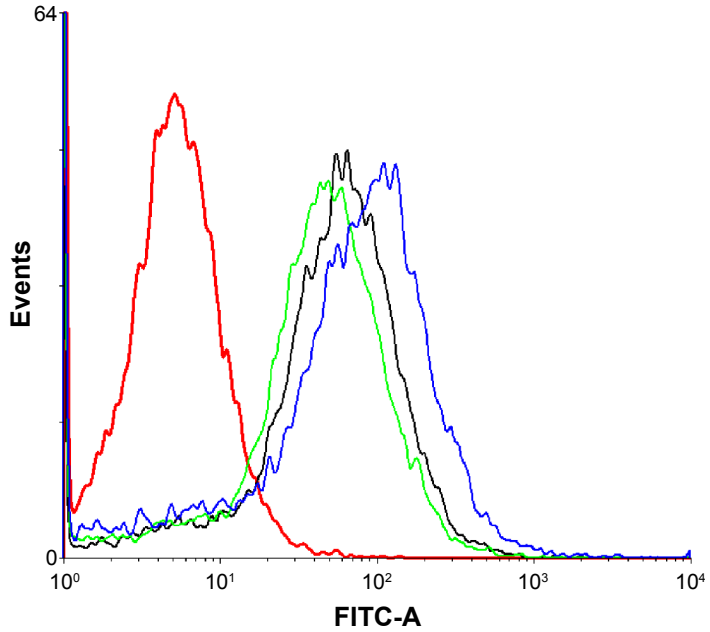

Figure S4 Flow cytometry results for internalization ability among the various M-MSN-based siRNA delivery systems 4 hours after incubation with SKOV3 cells.

Notes: Red line indicates without treatment with any type of particle; green line indicates M-MSN_FAM-siRNA@PEI-PEG; black line indicates M-MSN_FAM-siRNA@PEI; and blue line indicates M-MSN_FAM-siRNA@PEI-PEG-KALA.

Abbreviations: FAM, fluorescein amidite; FITC, fluorescein isothiocyanate; M-MSN, magnetic mesoporous silica nanoparticle; PEI, polyethylenimine; PEG, polyethylene glycol; KALA, a type of fusogenic peptide; siRNA, small interfering RNA.

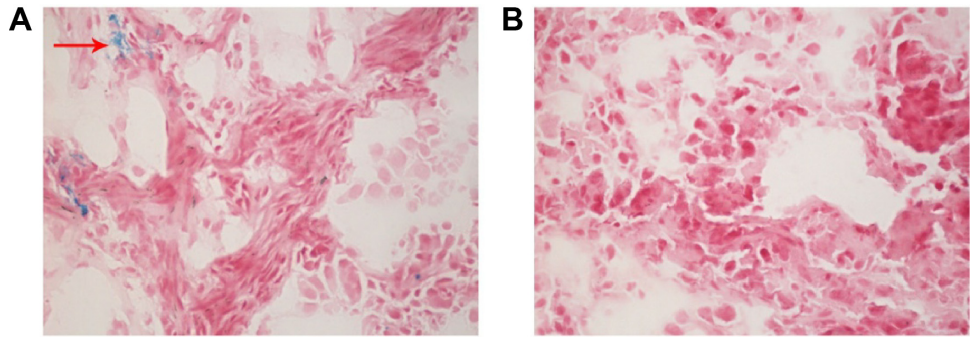

Figure S5 Iron from M-MSNs was revealed by Prussian blue staining.
Notes: (**A**) Tumor slide after injection of M-MSN_NC siRNA@PEI-PEG-KALA (red arrow points to the iron accumulated in tumor region). (**B**) Liver tissue from animals that were not injected with nanocarriers, but the equivalent saline. Magnification was 20×.
Abbreviations: M-MSN, magnetic mesoporous silica nanoparticles; PEI, polyethylenimine; PEG, polyethylene glycol; KALA, a type of fusogenic peptide; NC siRNA, negative control small interfering RNA.

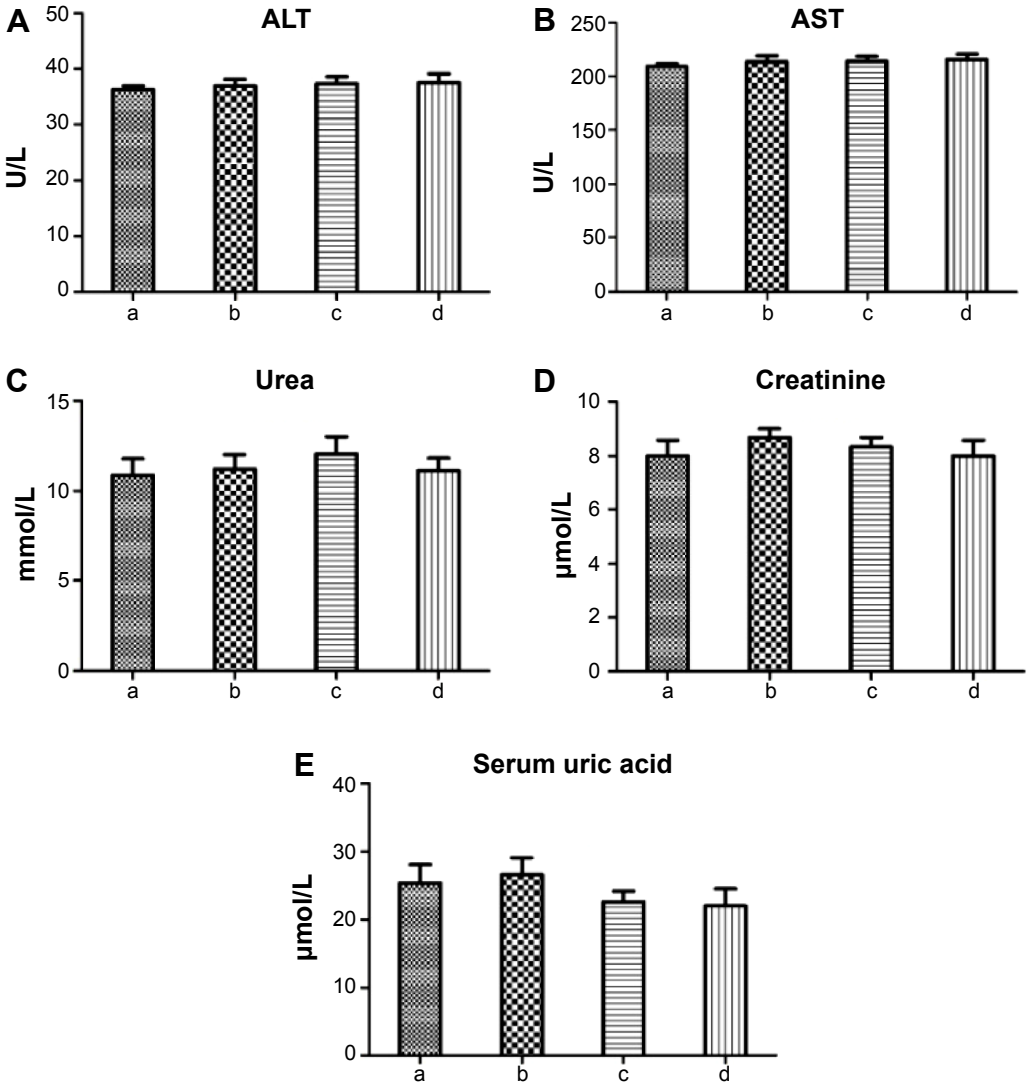

Figure S6 Safety and biocompatibility of M-MSN_VEGF siRNA@PEI-PEG-KALA.
Notes: Representative markers of nephrotoxicity and hepatotoxicity were evaluated, including ALT (**A**), AST (**B**), urea (**C**), creatinine (**D**), and serum uric acid (**E**). a: M-MSN_VEGF siRNA@PEI-PEG-KALA; b: M-MSN_NC siRNA@PEI-PEG-KALA; c: M-MSN@PEI-PEG-KALA; d: saline.
Abbreviations: ALT, alanine aminotransferase; AST, aspartate aminotransferase; M-MSN, magnetic mesoporous silica nanoparticle; PEI, polyethylenimine; PEG, polyethylene glycol; KALA, a type of fusogenic peptide; VEGF siRNA, vascular endothelial growth factor small interfering RNA.

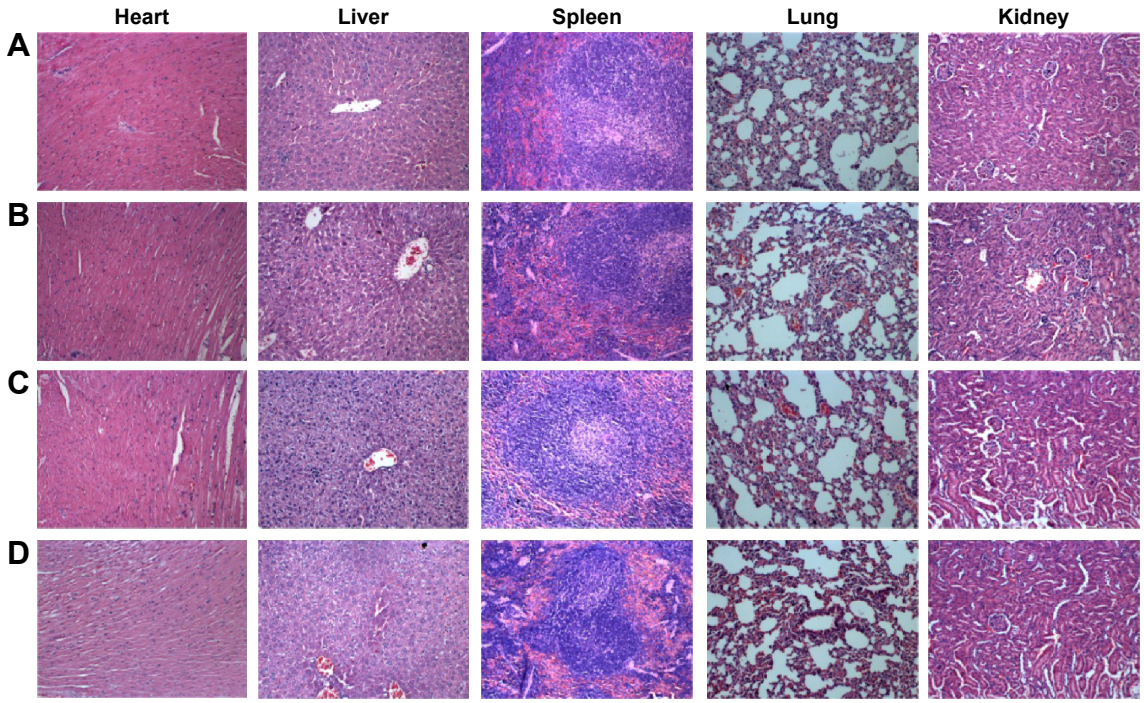

Figure S7 Hematoxylin and eosin staining of the major organs, including the heart, liver, spleen, lung, and kidney.
Notes: Magnification 20×. **A**: M-MSN_VEGF siRNA@PEI-PEG-KALA; **B**: M-MSN_NC siRNA@PEI-PEG-KALA; **C**: M-MSN@PEI-PEG-KALA; **D**: saline.
Abbreviations: M-MSN, magnetic mesoporous silica nanoparticle; NC, negative control; PEI, polyethylenimine; PEG, polyethylene glycol; KALA, a type of fusogenic peptide; VEGF siRNA, vascular endothelial growth factor small interfering RNA.

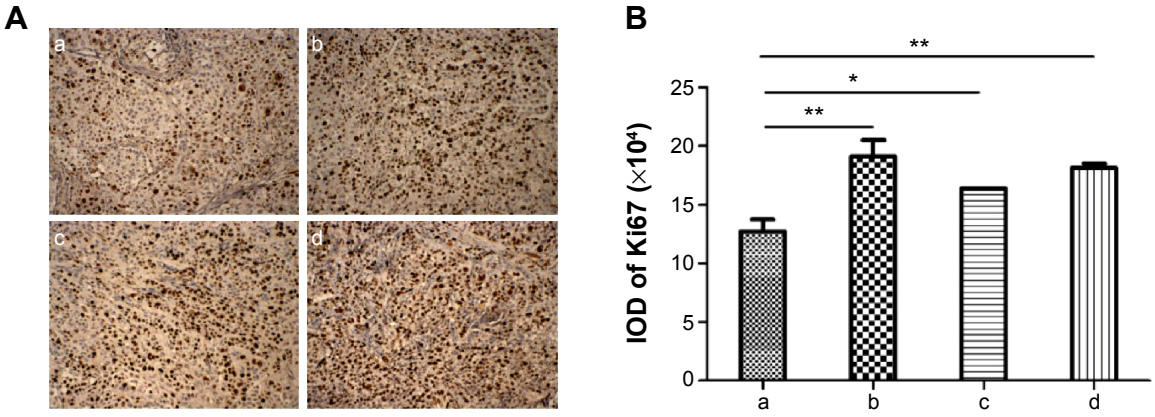

Figure S8 (**A**) Immunohistological analysis for Ki-67 expression in tumor sections from the four experimental groups. (**B**) Statistical analysis from immunohistological results.
Notes: Data are shown as the mean ± standard deviation. a: M-MSN_VEGF siRNA@PEI-PEG-KALA; b: M-MSN_NC siRNA@PEI-PEG-KALA; c: M-MSN@PEI-PEG-KALA; d: saline. (*$P<0.01$; **$P<0.001$; n=5). Magnification 20×.
Abbreviation: IOD, integral optical density.